IEEE Photonics Journal
An IEEE Photonics Society Publication

Open Access

Highly Efficient Tunable Dispersive Wave in a Tellurite Microstructured Optical Fiber

Volume 7, Number 1, February 2015

Tonglei Cheng
Dinghuan Deng
Xiaojie Xue
Lei Zhang
Takenobu Suzuki
Yasutake Ohishi

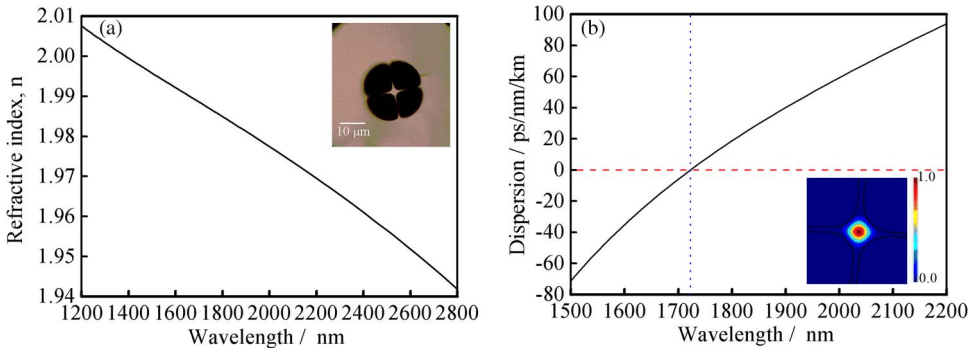

DOI: 10.1109/JPHOT.2014.2381662
1943-0655 © 2014 IEEE

IEEE photonics SOCIETY

IEEE

Highly Efficient Tunable Dispersive Wave in a Tellurite Microstructured Optical Fiber

Tonglei Cheng, Dinghuan Deng, Xiaojie Xue, Lei Zhang, Takenobu Suzuki, and Yasutake Ohishi

Research Center for Advanced Photon Technology, Toyota Technological Institute, Nagoya 468-8511, Japan

DOI: 10.1109/JPHOT.2014.2381662

Manuscript received October 19, 2014; revised November 25, 2014; accepted December 3, 2014. Date of current version December 30, 2014. This work was supported by MEXT: the Support Program for Forming Strategic Research Infrastructure (2011-2015). Corresponding author: T. Cheng (e-mail: chengtonglei@gmail.com).

Abstract: We demonstrate a highly efficient, stable, and tunable dispersive wave (DW) emitted by the soliton in a tellurite microstructured optical fiber. The dependence of the generated DW properties on the average pump power is experimentally investigated. By using the 80-MHz pulse emitted from an optical parametric oscillator as the pump source, the DW from ∼1626 to 1685 nm is obtained with the average pump power changing from ∼250 to 440 mW at the pump wavelength of ∼1760 nm. The conversion efficiency is over ∼65%. The full width at half maximum (FWHM) of DW pulse at the center wavelength of ∼1626 nm is ∼90 fs, which was measured by an intensity autocorrelator. The stable DW pulse can be used as a near-infrared femtosecond source.

Index Terms: Dispersive wave, tellurite microstructured optical fiber (TMOF), soliton.

1. Introduction

In nonlinear fiber optics, dispersive wave (DW) generation, which is also called Cherenkov radiation (CR) or nonsolitonic radiation, originates from the perturbation of a stable temporal soliton in the anomalous dispersion regime by the higher order fiber dispersion [1]–[4]. And DW has already been widely applied in the tunable femtosecond source and wavelength conversion [5], [6]. Recently, great attention has been devoted to DW in microstructured optical fibers (MOFs) which can offer controllable chromatic dispersion and high nonlinearity [7]–[10]. For the highly efficient DW, two conditions must be satisfied: Solitons and DW must share the same phase velocity, and the spectral tails of the soliton must overlap with the DW wavelength [11]–[13]. Although some reports have demonstrated the highly efficient DW in MOFs [14]–[19], the reported maximal conversion efficiency (η) was limited at ∼50% [11], and most of the research was based on silica fibers.

Soft-glass MOFs, fabricated by tellurite or chalcogenide glasses, have broad transparency ranges in the mid-infrared and high nonlinear refractive indices exceeding that of silica glass by at least one order of magnitude [20]–[22]. They have been widely applied in nonlinear fiber optics, such as supercontinuum (SC) generation, soliton self-frequency shift (SSFS), and third-harmonic generation (THG), etc. [23]–[5].

In the paper, a four-hole tellurite (76.5 TeO_2-6 Bi_2O_3-11.5 Li_2O-6 ZnO, mol%) MOF (TMOF) was designed and fabricated for the highly efficient and tunable DW generation. The diameter

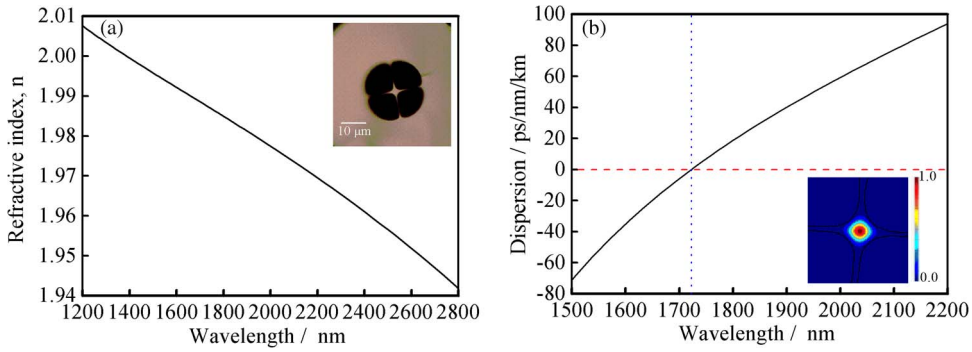

Fig. 1. Fundamental mode refractive index of the TMOF. (Inset) Cross section of the TMOF. (b) Calculated chromatic dispersion curve of the fundamental mode. (Inset) Fundamental mode-field profile at 1800 nm.

of the core was ~4.7 μm, and the loss was measured to be ~0.2 dB/m at ~1800 nm using the cutback method. Tunable DW from ~1685 to 1626 nm was obtained when the TMOF was pumped by an optical parametric oscillator (OPO) with the pump wavelength of ~1760 nm. The conversion efficiency was over ~65%. The 3 dB spectral bandwidth of DW increased from ~34 to 63 nm with the average pump power increasing from ~250 to 440 mW, and the full width at half maximum (FWHM) of the DW was ~90 fs pulse width with 440 mW, measured by an intensity autocorrelator. The generated DW pulse can be used as a tunable near-infrared femtosecond source.

2. Structure of TMOF

The inset of Fig. 1(a) shows the cross section of the TMOF observed by an optical microscope. The TMOF was fabricated by the rod-in-tube technique. The fundamental mode refractive index was calculated from 1200 to 2800 nm, and the core and cladding diameters were ~4.7 and ~128 μm, respectively. At the wavelength of ~1800 nm, the loss was ~0.2 dB/m measured by the cutback technique, and the calculated nonlinear coefficient was ~212 $km^{-1}W^{-1}$ based on the nonlinear refractive index of ~5.9×10^{-19} m^2W^{-1} for tellurite glass and the effective mode area of ~9.7 μm^2 [26]. The nonlinear refractive index of this tellurite glass was higher than some reports [27], [28] due to Bi_2O_3 in the composition. Fig. 1(b) shows the chromatic dispersion curve calculated by a commercial software (Lumerical MODE Solution) using the full-vectorial mode solver technology. The fundamental mode-field intensity at 1800 nm is shown in the inset of Fig. 1(b). We can see that the zero-dispersive wave (ZDW) of the TMOF was ~1720 nm.

3. Experimental Conditions and Results

The experimental setup for the DW generation in a 2 cm-long TMOF is shown in Fig. 2(a). The laser pulse tuned from 1700 nm to 3000 nm with the repetition rate of ~80 MHz generated from an OPO (Coherent Inc.) was used as the pump source. The FWHM of laser pulse was ~560 fs, which was measured by an intensity autocorrelator. The mode field profile of the propagation beam from the OPO at ~1800 nm was measured by a CCD camera, as shown in Fig. 2(b). After a neutral density (ND) filter, the pulse was coupled into the core of the TMOF by a lens with the focus length of ~4.0 mm and the numerical aperture (NA) of ~0.56 (THORLABS, CO36TME-D). The output signal was then butt-coupled into a 0.3 m long large-mode-area (LMA) fluoride (ZBLAN) fiber with the core diameter of ~105 μm and the transmission window from 0.4 to 5 μm. The nonlinear effect in ZBLAN fiber could be ignored due to the large core size. Finally, the LMA ZBLAN fiber was connected to an optical spectrum analyzer (OSA, 1200-2400 nm) to record the DW signal.

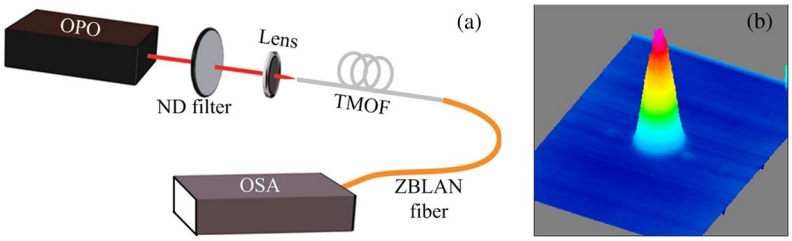

Fig. 2. (a) Experimental setup for DW generation in the TMOF. (b) Mode field profile intensity at ~1800 nm.

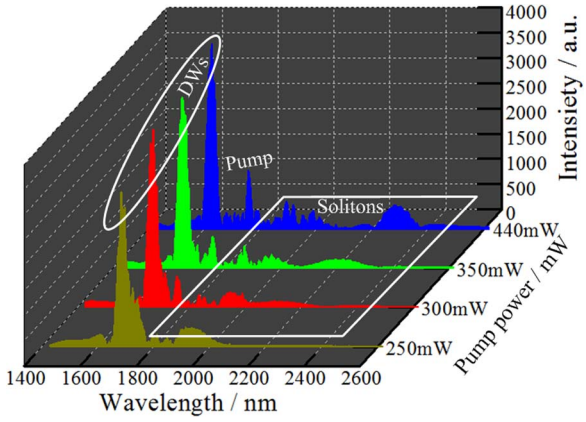

Fig. 3. DW evolution with the average pump power at ~250, 300, 350, and 440 mW.

First, we used the pump wavelength $\lambda_{\text{pump}} = 1760$ nm, which was in the anomalous dispersion regime and close to the ZDW of the TMOF. The average power measured after the lens was ~250, 300, 350, and 440 mW. The coupling efficiency was ~24%, which was defined as the ratio between the power transmitting in the core and the power before the lens. Because only a little power leaked into the cladding, which can be neglected, the power transmitting in the core can be measured by OSA from the output end of the TMOF. Considering the coupling efficiency, the peak power launched into the fiber was calculated to be ~1.34, 1.61, 1.88, and 2.36 kW. Fig. 3 shows DW evolution with the increase of the average pump power. And the center wavelength of the fundamental soliton was changed from ~1920 to 2280 nm. The evolution of the red-shifted spectrum was mainly ruled by the fact that the input pulse behaved as solitons which underwent a fission process during propagation in the TMOF, whereas the blue-shifted radiation mainly originated from DW which was determined by the phase-matching condition. In our experiments, when the ~1760 nm pump power increased from ~250 to 440 mW, the center wavelength of the emitted DW shifted from ~1685 to 1626 nm, yielding a blueshift in this process. The 3 dB spectral bandwidth increased from ~34 to 63 nm with the change of the average pump power. At the average pump power of ~440 mW, DW with the center wavelength of ~1626 nm was emitted by the fundamental soliton with the center wavelength of ~2280 nm.

The wavelength location of DW is predicted by a phase-matching condition [2]

$$\sum_{n\geq 2} \frac{\beta_n(\omega_S)}{n!}(\omega_{DW} - \omega_S)^n = \frac{\gamma P_S}{2} \tag{1}$$

where $\beta_n(\omega_S)$ is the nth derivative of the dispersion coefficient at the soliton frequency, and $n = 6$ is considered in the paper. ω_S and P_S are the center frequency and peak power of the soliton, respectively. ω_{DW} is the center frequency of DW, and γ is the nonlinear coefficient. Physically,

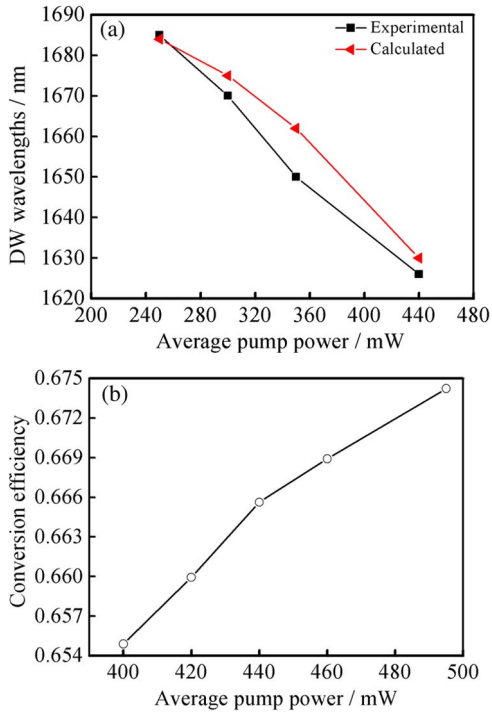

Fig. 4. (a) Calculated and experimental center wavelengths of DW with the average pump power at ~250, 300, 350, and 440 mW. (b) DW conversion efficiency with the average pump power at ~400, 420, 440, and 495 mW.

when the third order dispersion $\beta_3 > 0$, ω_{DW} is larger than ω_S, and DW shifts to the blue-shifted region. Based on the phase-matching condition, the calculated and experimental center wavelengths of DW with different average pump power were shown in Fig. 4(a). The discrepancy was limited within the range of ~12 nm, which was induced by the instability of the soliton and the nonlinear phase shift [10], [29]. The DW conversion efficiency as a function of the average pump power measured by OSA was shown in Fig. 4(b), which was defined as the ratio between the DW power and the total pump power at the output end of the TMOF and adapted in [30]. The conversion efficiency grew monotonously with the average pump power, and reached $\eta = 67.4\%$ at ~495 mW, which exceeded the highest value ever reported. Such a high efficiency can be explained as follow. Under the combined effect of the self-phase modulation (SPM) and dispersion, the input pulse was compressed in the first phase and its spectrum overlapped the resonant wavelength. Consequently, an effective wide bandwidth DW was gained. The prior DW was amplified as a seed by the soliton, and then developed into a more energetic DW [17]. However, there are other two potential reasons. One was the high nonlinear refractive index of the tellurite glass compared with the silica glass. As a result, γ P will be large and the phase-matching condition can be satisfied in the wide wavelength range. The other was the pump wavelength closed to the ZDW, which mean that the dispersion term of (1) was nearly zero. Thus the phase-matching condition can be satisfied with the low pump power.

In order to characterize the temporal profile of the generated DW pulse, the FWHM was measured by an intensity autocorrelator. Because the 3 dB spectral bandwidth of the generated DW changed with pump power, the FWHM also changed. The generated DW pulse width with the center wavelength of ~1626 nm was measured at the average pump power of ~440 mW, as shown in Fig. 5. The FWHM of the pump pulse at ~1760 nm was ~560 fs, whereas the FWHM of the generated DW pulse was ~90 fs. The latter was more than six times shorter due to the pump pulse compression in the TMOF. The dispersion length $L_D = T_{0^2}/|\beta_2|$. At the center wavelength of DW (~1626 nm), $T_0 \approx T_{\mathrm{FWHM}}/1.763$ is the pulse width for hyperbolic-secant shape,

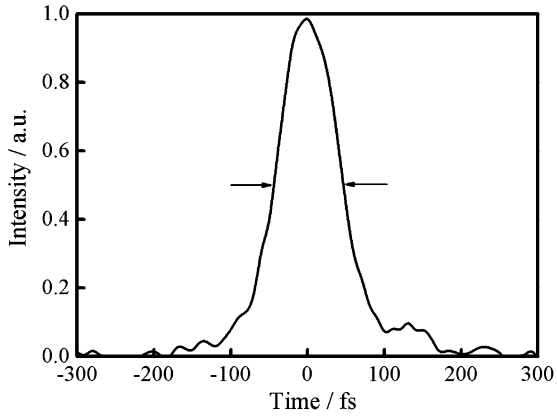

Fig. 5. FWHM of the generated DW pulse with the center wavelength of ∼1626 nm measured by the intensity autocorrelator.

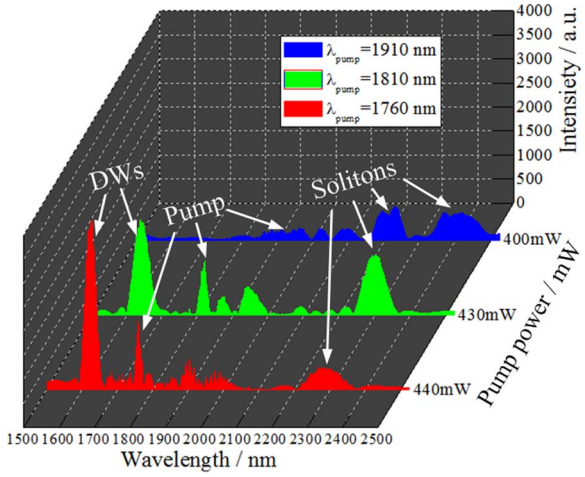

Fig. 6. Generated DW with the pump wavelength at ∼1760, 1810, and 1910 nm.

and $T_0 = 51$ fs. $\beta_2 = 33.5$ ps^2/km is the dispersion parameter calculated according to Fig. 1(b). The calculated $L_D = \sim 7.8$ cm and $L_D \geq L = 2$ cm. As a result, the dispersion-induced broadening of the DW pulse can be neglected and the pulse can be considered stable. On the other hand, the 3 dB spectral bandwidth was ∼63 nm $(\sim 1596 - 1659$ nm$)$, and based on this the calculated actual pulse width of DW pulse was ∼61 fs (transform-limit), which was shorter than the measured FWHM value (∼90 fs). One of the reasons was that the DW pulse was connected with the intensity autocorrelator by a 10 cm-long single mode fiber (SMF) and during the transmission in the SMF, the pulse was slightly broadened. Considering the coupling and conversion efficiency, the output peak power of DW was ∼9.8 kW, which was higher than the launched peak pump power (∼2.36 kW). This is because the pulse was compressed to ∼90 fs, and from this we can see that the highly efficient and stable DW with the tunable range of ∼59 nm can be used as a femtosecond source.

In order to show the generated DW as a function of the pump wavelength, DW at the pump wavelength of ∼1760, 1810, and 1910 nm was investigated with different powers, as shown in Fig. 6. With the increase of the pump wavelength and the further away from the ZDW, the conversion efficiency decreased. At $\lambda_{\text{pump}} = 1760$ nm with the average power of ∼440 mW, $\eta = 66.6\%$. At $\lambda_{\text{pump}} = 1810$ nm with the average power of ∼430 mW, $\eta = 32.7\%$, and at $\lambda_{\text{pump}} = 1910$ nm with the average power of ∼400 mW, no obvious DW peak appeared in the blue-shifted

region, and most of the pump power shifted to the solitons. This is due to the fact that the pump wavelength ∼1910 nm was far away from the ZDW, thus according to (1) the phase-matching condition cannot be satisfied.

4. Summary

In summary, we designed and fabricated a four-hole TMOF for the highly efficient and tunable DW generation. A stable DW pulse from ∼1626 to 1685 nm was obtained with the average pump power increasing from ∼250 to 440 mW at the pump wavelength of ∼1760 nm. The 3 dB spectral bandwidth of DW increased from ∼34 to 63 nm, and the FWHM of DW was ∼90 fs at the average pump power of ∼440 mW, which was more than six times shorter than that of the pump pulse. Furthermore, the conversion efficiency can reach ∼67.4% at the average pump power of ∼495 mW. The highly efficient, stable and tunable DW generated in the TMOF can be us ed as a near-infrared femtosecond source.

References

[1] N. Akhmediev and M. Karlsson, "Cherenkov radiation emitted by solitons in optical fibers," *Phys. Rev. A*, vol. 51, pp. 2602–2607, Mar. 1995.
[2] G. P. Agrawal, *Nonlinear Fiber Optics*, 4th ed. New York, NY, USA: Academic, 2007.
[3] P. K. A. Wai, C. R. Menyuk, Y. C. Lee, and H. H. Chen, "Nonlinear pulse propagation in the neighborhood of the zero-dispersion wavelength of monomode optical fibers," *Opt. Lett.*, vol. 11, no. 7, pp. 464–466, Jul. 1986.
[4] A. C. Judge, O. Bang, and C. M. de Sterke, "Theory of dispersive wave frequency shift via trapping by a soliton in an axially nonuniform optical fiber," *J. Opt. Soc. Am. B*, vol. 27, no. 11, pp. 2195–2202, Nov. 2010.
[5] M. L. Hu, C. Y. Wang, L. Chai, and A. M. Zheltikov, "Frequency-tunable anti-Stokes line emission by eigenmodes of a birefringent microstructure fiber," *Opt. Exp.*, vol. 12, no. 9, pp. 1932–1937, May 2004.
[6] X. M. Liu *et al.*, "All-fiber femtosecond Cherenkov radiation source," *Opt. Lett.*, vol. 37, no. 13, pp. 2769–2771, Jul. 2012.
[7] S. Roy, S K. Bhadra, and G. P. Agrawal, "Dispersive wave generation in supercontinuum process inside nonlinear microstructured fibre," *Current Sci.*, vol. 100, no. 3, pp. 321–342, Feb. 2011.
[8] N. Karasawa and K. Tada, "The generation of dispersive waves from a photonic crystal fiber by higher-order mode excitation," *Opt. Exp.*, vol. 18, no. 5, pp. 5338–5343, Mar. 2010.
[9] W. B. Wang, H. Yang, P. H Tang, C. J. Zhao, and J. Gao, "Soliton trapping of dispersive waves in photonic crystal fiber with two zero dispersive wavelengths," *Opt. Exp.*, vol. 21, no. 9, pp. 11 215–11 226, May 2013.
[10] I. Cristiani, R. Tediosi, L. Tartara, and V. Degiorgio, "Dispersive wave generation by solitons in microstructured optical fibers," *Opt. Exp.*, vol. 12, no. 1, pp. 124–135, Jan. 2004.
[11] G. Manili *et al.*, "Gigantic dispersive wave emission from dual concentric core microstructured fiber," *Opt. Lett.*, vol. 37, no. 19, pp. 4101–4103, Oct..2012.
[12] H. Tu and S. A. Boppart, "Optical frequency up-conversion by supercontinuum-free widely-tunable fiber-optic Cherenkov radiation," *Opt. Exp.*, vol. 17, no. 12, pp. 9858–9872, Jun. 2009.
[13] S. Roy, S. K. Bhadra, and G. P. Agrawal, "Effects of higher-order dispersion on resonant dispersive waves emitted by solitons," *Opt. Lett.*, vol. 34, no. 13, pp. 2072–2074, Jul. 2009.
[14] J. H. Yuan *et al.*, "Coherent anti-Stokes Raman scattering microscopy by dispersive wave generations in a polarization maintaining photonic crystal fiber," *IEEE Photon. Technol. Lett.*, vol. 23, no. 12, pp. 786–788, Jun. 2011.
[15] G. Q. Chang, L. J. Chen, and F. X. Kärtner, "Highly efficient Cherenkov radiation in photonic crystal fibers for broadband visible wavelength generation," *Opt. Lett.*, vol. 35, no. 14, pp. 2361–2363, Jul. 2010.
[16] M. Erkintalo, G. Genty, and J. M. Dudley, "Giant dispersive wave generation through soliton collision," *Opt. Lett.*, vol. 35, no. 5, pp. 658–660, Mar. 2010.
[17] X. B. Zhang *et al.*, "Enhanced violet Cherenkov radiation generation in GeO2-doped photonic crystal fiber," *Appl. Phys. B*, vol. 111, no. 2, pp. 273–277, May 2013.
[18] H. H. Tu *et al.*, "Bright broadband coherent fiber sources emitting strongly blue-shifted resonant dispersive wave pulses," *Opt. Exp.*, vol. 21, no. 20, pp. 23 188–23 196 Oct. 2013.
[19] F. R. Arteaga-Sierra *et al.*, "Multi-peak-spectra generation with Cherenkov radiation in a non-uniform single mode fiber," *Opt. Exp.*, vol. 22, no. 3, pp. 2451–2458, Feb. 2014.
[20] T. L. Cheng *et al.*, "Soliton self-frequency shift and third-harmonic generation in a four-hole As_2S_5 microstructured optical fiber," *Opt. Exp.*, vol. 22, no. 4, pp. 3740–3746, Feb. 2014.
[21] G. Qin *et al.*, "Second and third harmonics and flattened supercontinuum generation in tellurite microstructured fibers," *Opt. Lett.*, vol. 35, no. 1, pp. 58–60, Jan. 2010.
[22] M. S. Liao *et al.*, "Five-order SRSs and supercontinuum generation from a tapered tellurite microstructured fiber with longitudinally varying dispersion," *Opt. Express*, vol. 19, no. 16, pp. 15 389–15 396, Aug. 2011.
[23] M. S. Liao, G. S. Qin, X. Yan, T. Suzuki, and Y. Ohishi, "A Tellurite nanowire with long suspended struts for low threshold single-mode supercontinuum generation," *J. Lightw. Technol.*, vol. 29, no. 2, pp. 194–199, Jan. 2011.
[24] T. L. Cheng *et al.*, "Soliton self-frequency shift and dispersive wave in a hybrid four-hole $AsSe_2 - As_2S_5$ microstructured optical fiber," *Appl. Phys. Lett.*, vol. 104, no. 12, Mar. 2014, Art. ID. 121911.
[25] T. L. Cheng *et al.*, "Tunable third-harmonic generation in a chalcogenide-tellurite hybrid optical fiber with high refractive index difference," *Opt. Lett.*, vol. 39, no. 4, pp. 1005–1007, Feb. 2014.

[26] M. Liao *et al.*, "Fabrication and characterization of a chalcogenide-tellurite composite microstructure fiber with high nonlinearity," *Opt. Exp.*, vol. 17, no. 24, pp. 21 608–21 614, Nov. 2009.
[27] P. Domachuk *et al.*, "Over 4000 nm bandwidth of mid-IR supercontinuum generation in sub-centimeter segments of highly nonlinear tellurite PCFs," *Opt. Exp.*, vol. 16, no. 10, pp. 7161–7168, May 2008.
[28] A. Lin, A. Zhang, E. J. Bushong, and J. Toulouse, "Solid-core tellurite glass fiber for infrared and nonlinear applications," *Opt. Exp.*, vol. 17, no. 19, pp. 16 716–16 721, Sep. 2009.
[29] L. Zhang, S. G. Yang, Y. Han, H. W. Chen, M. H. Chen, and S. Z. Xie, "Simultaneous generation of tunable giant dispersive waves in the visible and mid-infrared regions based on photonic crystal fibers," *J. Opt.*, vol. 15, no. 7, Jul. 2013, Art. ID. 075201.
[30] M. C. Chan, C. H. Lien, J. Y. Lu, and B. H. Lyu, "High power NIR fiber-optic femtosecond Cherenkov radiation and its application on nonlinear light microscopy," *Opt. Exp.*, vol. 22, no. 8, pp. 9498–9507, Apr. 2014.